

NMR Structure Determination of Protein–Ligand Complexes by Lanthanide Labeling

GUIDO PINTACUDA,[§] MICHAEL JOHN,
XUN-CHENG SU, AND GOTTFRIED OTTING*
*Research School of Chemistry, Australian National University,
Canberra, ACT 0200, Australia*

Received August 2, 2006

ABSTRACT

The paramagnetism of lanthanide ions offers outstanding opportunities for fast determinations of the three-dimensional (3D) structures of protein–ligand complexes by nuclear magnetic resonance (NMR) spectroscopy. It is shown how the combination of pseudocontact shifts (PCSs) induced by a site-specifically bound lanthanide ion and prior knowledge of the 3D structure of the lanthanide-labeled protein can be used to achieve (i) rapid assignments of NMR spectra, (ii) structure determinations of protein–protein complexes, and (iii) identification of the binding mode of low-molecular weight compounds in complexes with proteins. Strategies for site-specific incorporation of lanthanide ions into proteins are summarized.

Introduction

Three-dimensional (3D) structures of proteins are determined by X-ray crystallography and NMR spectroscopy at an ever increasing rate. Yet, the structure determination of protein–protein and, more generally, protein–ligand complexes is often less straightforward, either because they defy crystallization or because their molecular weight is too large for complicated NMR experiments. Therefore, simple methods for defining the relative position and orientation of two molecules in a protein–ligand complex would be of great value. This Account describes lan-

thanide-based NMR methods to achieve this for proteins of known 3D structure with a specific lanthanide binding site.

For the NMR spectroscopist, lanthanides stand out for their large and varied paramagnetism arising from unpaired electrons in the f orbitals of their trivalent ions. The paramagnetism gives rise to pronounced changes in chemical shifts of the nuclear spins located nearby.^{1,2} This effect has been widely exploited in organic chemistry to resolve overlapping NMR signals of compounds with the help of lanthanide-induced shifts.^{3–6}

The effects of paramagnetic metal ions on NMR spectra are well understood and can be described mathematically.⁷ Paramagnetic metal ions cause not only paramagnetic shifts but also enhanced nuclear relaxation, molecular alignment in the magnetic field, and various cross-correlation effects.^{7–11} Among these, paramagnetic shifts convey particularly useful long-range structural information and are easily measured with high accuracy. Consequently, they have long been used for structure determinations by NMR spectroscopy,^{12–16} including 3D structure determinations of paramagnetic metalloproteins.^{17–20}

Lanthanides form stable trivalent ions without any known essential role in biology. Yet, Ca²⁺ ions of calcium-binding proteins can be substituted by lanthanide ions, embedding the lanthanide ion (Ln³⁺) in a rigid and extended molecular framework of defined three-dimensional structure.^{13,21} In this way, detailed information about the spatial anisotropy of the paramagnetic effects induced by different lanthanide ions has been obtained²² without the extensive motional averaging usually encountered in complexes with lanthanide shift reagents. A growing number of recent studies confirms the potential of lanthanides for NMR applications in structural biology.^{20,23–28} As one of their most important features, lanthanides allow the modulation of the paramagnetic effects by exchange of one lanthanide for another, since Ln³⁺ ions are chemically similar yet paramagnetically varied. In particular, diamagnetic lanthanide ions provide an excellent diamagnetic reference, allowing the measurement of the paramagnetic shifts simply as the difference in chemical shifts observed in the presence of a paramagnetic or diamagnetic lanthanide. Finally, the unpaired electrons reside in inner orbitals with little overlap with the ligand field, making contact shifts negligible in most situations and allowing the interpretation of paramagnetic shifts as pseudocontact shifts.¹²

The following overview focuses on the use of pseudocontact shifts induced by lanthanide ions for structure determinations of protein–protein and protein–ligand complexes from a small set of NMR data. It is shown how detailed structural information can be derived from straightforward 1D and 2D NMR spectra, which can be recorded with acceptable sensitivity also in the case of

Guido Pintacuda completed his Ph.D. in chemistry from the Scuola Normale in Pisa, Italy, in 2000. His postdoctoral work (2001–2005) at the Karolinska Institute and at the Australian National University focused on the use of paramagnetic metal ions for applications in structural biology by NMR spectroscopy. He is currently an associate scientist of the French National Center for Scientific Research (CNRS). He works at the Ecole Normale Supérieure de Lyon where he investigates paramagnetic proteins by solid-state NMR spectroscopy.

Michael John received his Ph.D. in chemistry from the Technical University of Munich, Germany, in 2004. He is currently a Feodor Lynen fellow focusing on the paramagnetic effects of lanthanide ions for the study of the interaction between proteins and small ligand molecules.

Xun-Cheng Su received his Ph.D. in chemistry from Nankai University in 2001, Tianjin, China. His postdoctoral work at the University of Florence, Italy (2001–2004), focused on 3D structure determinations of metalloproteins by NMR spectroscopy. His current work involves chemical tagging of proteins with lanthanide ions and structure determinations.

Gottfried Otting received his Ph.D. in biophysics from the Eidgenössische Technische Hochschule in Zürich, Switzerland, with Kurt Wüthrich in 1987. He continued as a research fellow in the same laboratory until he was appointed professor of molecular biophysics at the Karolinska Institute in Stockholm, Sweden, in 1992. He moved to the Australian National University in 2002 on a Federation Fellowship by the Australian Research Council. His research interest is the development of technologies for the application of NMR spectroscopy in structural biology.

* Corresponding author. Tel: 0061 2 6125 6507. Fax: 0061 2 6125 0750. E-mail: gottfried.otting@anu.edu.au.

[§] Present address: Ecole Normale Supérieure de Lyon, Laboratoire de Chimie, 46 Allée d'Italie, 69364 Lyon, France.

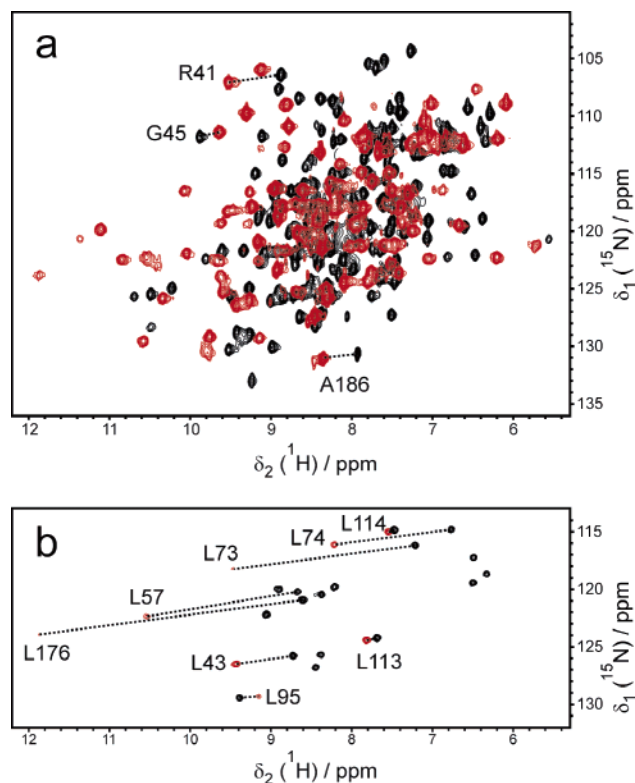


FIGURE 1. Superposition of ^{15}N HSQC spectra recorded of the protein complex $\epsilon 186/\theta$ loaded with Tb^{3+} and La^{3+} . The cross-peaks are from the amides of the 185-residue protein $\epsilon 186$, which was labeled with ^{15}N : (a) spectra recorded with uniformly ^{15}N -labeled $\epsilon 186$; (b) spectra recorded with $\epsilon 186$ selectively labeled with ^{15}N -leucine. The diamagnetic spectrum recorded with La^{3+} is plotted in black. The paramagnetic spectrum recorded with Tb^{3+} is plotted in red. Selected paramagnetic/diamagnetic peak pairs are connected by lines and labeled with the assignment of the peaks to specific residues in the protein.

high-molecular weight systems, and how lanthanide ions can be site-specifically attached to otherwise diamagnetic proteins.

Pseudocontact Shifts from Lanthanide Ions

The pseudocontact shifts (PCSs) induced by a lanthanide ion can be pronounced (Figure 1). For some paramagnetic lanthanide ions, PCSs can be measured for nuclear spins as far as 40 Å from the metal ion.^{23,29} PCSs arise from through-space interactions with the unpaired electrons of the paramagnetic center. It is informative to visualize the PCSs as shells of constant PCS value (“isosurfaces”) plotted on the protein structure (Figure 2a). This shows that the PCS value observed for any particular nuclear spin depends on the spatial location of the spin with respect to the paramagnetic metal ion.

The spatial PCS distribution shown in Figure 2a is described by

$$\Delta\delta^{\text{PCS}} = \frac{1}{12\pi r^3} \left[\Delta\chi_{\text{ax}} (3 \cos^2 \theta - 1) + \frac{3}{2} \Delta\chi_{\text{rh}} \sin^2 \theta \cos 2\varphi \right] \quad (1)$$

where $\Delta\delta^{\text{PCS}}$ denotes the difference in chemical shifts

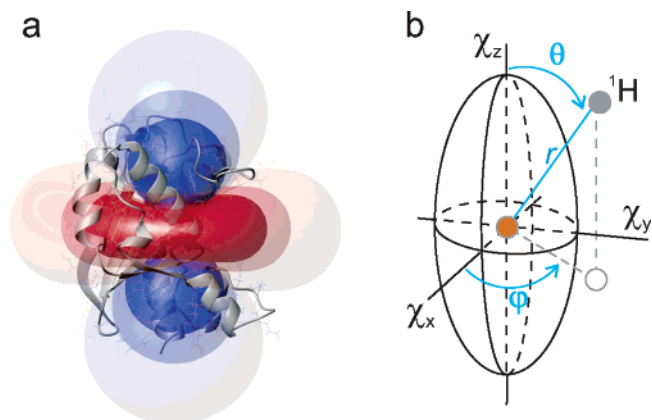


FIGURE 2. (a) Isosurfaces depicting the pseudocontact shifts (PCSs) induced by Dy^{3+} plotted on a ribbon representation of the crystal structure³⁷ of $\epsilon 186$. Blue and red surfaces identify the spatial locations of positive and negative PCSs, respectively, by ± 3 , ± 1.5 , and ± 0.5 ppm. The PCS isosurfaces constitute a representation of the $\Delta\chi$ tensor. (b) Schematic representation of the χ tensor, illustrating the electron–nucleus distance r (the nuclear spin being exemplified by a ^1H) and the angles θ and φ (eq 1).

measured between diamagnetic and paramagnetic samples, r is the distance between the metal ion and the nuclear spin, $\Delta\chi_{\text{ax}}$ and $\Delta\chi_{\text{rh}}$ are the axial and rhombic components of the $\Delta\chi$ tensor, and the angles θ and φ describe the position of the nuclear spin with respect to the principal axes of the $\Delta\chi$ tensor.

The $\Delta\chi$ tensor is the anisotropy component of the magnetic susceptibility tensor χ of the metal ion. The χ tensor governs all paramagnetic effects. It can be viewed as an ellipsoid spanned by the three principal axes, χ_x , χ_y , and χ_z , centered about the metal ion and fixed with respect to the molecular frame of the protein (Figure 2b). The anisotropic components, $\Delta\chi_{\text{ax}}$ and $\Delta\chi_{\text{rh}}$, of the $\Delta\chi$ tensor are given by $\Delta\chi_{\text{ax}} = \chi_z - (\chi_x + \chi_y)/2$ and $\Delta\chi_{\text{rh}} = \chi_x - \chi_y$. The χ and $\Delta\chi$ tensors share the same axis system, which also defines the symmetry axes of the isosurfaces shown in Figure 2a. In macromolecules and for metal ions with anisotropic χ tensor, the nuclear relaxation enhancements observed near the paramagnetic center are determined by the magnitude of the χ tensor. In contrast, only a nonvanishing $\Delta\chi$ tensor generates PCS. Most importantly, PCS measurements readily identify the Cartesian coordinate system defined by the $\Delta\chi$ tensor of a site-specifically attached lanthanide ion. This coordinate system thus presents a reference frame with respect to which both the protein and any binding partner can accurately be positioned using the geometric and distance dependence of the PCS effects (eq 1). Combined with the long-range nature of PCSs, this opens many unique opportunities in structural biology.

Comparison of Lanthanide Ions

The radius of trivalent lanthanide ions decreases uniformly with increasing atomic number from La^{3+} (1.17 Å) to Lu^{3+} (1.00 Å). Due to the similar size of different Ln^{3+} ions, a Ln^{3+} binding site of a protein can bind different lanthanides with similar, although not identical, affinities,^{30,31}

| | f1 | f2 | f3 | f5 | f6 | f7 | f8 | f9 | f10 | f11 | f12 | f13 |
|--|------------|--------------|-------------|------------|----------|-------------|------------|--------------|-----------|--------------|-----------|-------------|
| | Cerium | Praseodymium | Neodymium | Samarium | Europium | Gadolinium | Terbium | Dysprosium | Holmium | Erbium | Thulium | Ytterbium |
| J | Ce | Pr | Nd | Sm | Eu | Gd | Tb | Dy | Ho | Er | Tm | Yb |
| $\chi / 10^{-32} \text{ m}^3$ | 5/2 5.6 | 4 11.2 | 9/2 11.4 | 5/2 0.6 | 0 ~6 | 7/2 55.1 | 6 82.7 | 15/2 99.2 | 8 98.5 | 15/2 80.3 | 6 50.0 | 7/2 18.0 |
| PRE | | | | | | | | | | | | |
| $\Delta\chi_{ax} / 10^{-32} \text{ m}^3$ | 2.1 | 3.4 | 1.7 | 0.2 | -2.3 | 0 | 42.1 | 34.7 | 18.5 | -11.6 | -21.9 | -8.3 |
| $\Delta\chi_{rh} / 10^{-32} \text{ m}^3$ | 0.7 | 2.1 | 0.4 | -0.1 | -1.6 | 0 | 11.2 | 20.3 | 5.8 | -8.6 | -20.1 | -5.8 |
| PCS | | | | | | | | | | | | |
| τ_e / s | 10^{-13} | | | | | 10^{-7} | 10^{-13} | | | | | |

FIGURE 3. Paramagnetic properties of Ln^{3+} ions. Only paramagnetic and nonradioactive lanthanides are included. Representative isosurfaces are plotted for PCSs by ± 5 ppm using tensors reported by Bertini et al.²² The radius of the yellow sphere indicates the distance from the metal ion at which ^1H NMR signals of macromolecules with a rotational correlation time of 15 ns broaden by 80 Hz due to paramagnetic relaxation enhancement (PRE) at a magnetic field strength of 18.8 T. Typical electronic relaxation times representative for this field strength⁵² are indicated at the bottom. For Eu^{3+} , the estimate of the relaxation enhancement includes a contribution from excited J manifolds.²

and the 3D structure of the protein is only minimally disturbed when samples are prepared with paramagnetic and diamagnetic lanthanides. La^{3+} and Lu^{3+} provide suitable diamagnetic references, as well as Y^{3+} , which is not a lanthanide but is chemically closely related. The ion radius of Y^{3+} is the same as that of Dy^{3+} .

All lanthanide ions except La^{3+} and Lu^{3+} are paramagnetic. An overview over their paramagnetic properties is presented by Figure 3. Gd^{3+} is the only paramagnetic lanthanide with an isotropic environment of the unpaired electrons, resulting in a long electronic relaxation time that gives rise to strong relaxation enhancements in the NMR spectrum without significant changes in chemical shifts. Due to their outstanding relaxation enhancing properties, Gd^{3+} compounds are the most frequently used paramagnetic contrast agents in clinical MR imaging³² and have found applications as probes of solvent accessibility of protein surfaces.³³ In contrast, the electronic relaxation times of all other paramagnetic Ln^{3+} ions are very short due to nonisotropic populations of f-orbitals with unpaired electrons, which lead to low-lying excited states. In turn, the presence of low-lying excited states leads to strong magnetic anisotropy and fast electron relaxation, resulting in pronounced PCSs and less ^1H relaxation enhancement.

Since paramagnetic relaxation enhancements decrease with $1/r^6$ and PCSs decrease with $1/r^3$ (where r is the distance of the nuclear spin from the paramagnetic center), PCSs are readily observable for nuclear spins that are sufficiently far from the paramagnetic center to escape strong paramagnetic relaxation enhancements. For example, the paramagnetism of Dy^{3+} makes it difficult to observe ^1H NMR signals from protons within about 14 Å

from the Dy^{3+} ion, but PCSs are measurable within about 40 Å. Less paramagnetic lanthanides, such as Ce^{3+} , cause smaller PCSs and less relaxation, allowing the measurement of PCSs much closer to the metal ion. The choice of lanthanide thus provides a mechanism for tuning the paramagnetic effect to the distance range of interest.²⁹

Determination of the $\Delta\chi$ Tensor and Assignment of the Paramagnetic ^{15}N – ^1H Correlation

The position and magnitude of the $\Delta\chi$ tensor with respect to the protein is determined by only eight parameters: the values of $\Delta\chi_{ax}$ and $\Delta\chi_{rh}$, three angles defining the orientation of the $\Delta\chi$ tensor with respect to the coordinate system of the protein, and the x , y , and z coordinates of the metal ion. Therefore, as few as eight measured PCS values are sufficient to position the $\Delta\chi$ tensor with respect to the protein, provided it is known where the corresponding nuclear spins are located in the 3D structure of the protein.

^{15}N heteronuclear single quantum coherence (HSQC) spectra like those of Figure 1 correlate the chemical shifts of directly bonded ^1H and ^{15}N spins. The cross-peaks can be assigned to the amide groups of individual residues. Due to the spatial proximity of the ^1H and ^{15}N spin in an amide group, both spins experience very similar PCSs. Therefore, each cross-peak in the paramagnetic spectrum is displaced from its position in the diamagnetic spectrum by very similar ppm values in both dimensions. This displacement along diagonal lines greatly facilitates the identification of paramagnetic–diamagnetic peak pairs and presents the easiest route to transferring the cross-

peak assignments in the diamagnetic ^{15}N HSQC spectrum to a corresponding paramagnetic ^{15}N HSQC spectrum.

Provided the 3D structure of the protein and the resonance assignments of the diamagnetic ^{15}N HSQC spectrum are known, the assignment of the paramagnetic NMR spectrum can be supported by determination of the $\Delta\chi$ tensor and prediction of the PCSs of the remaining peaks using eq 1. This process has been implemented in the program Echidna,³⁴ which is capable of automatic assignment of most paramagnetic cross-peaks in a ^{15}N HSQC spectrum such as that shown in Figure 1a, including simultaneous automatic determination of the $\Delta\chi$ tensor parameters. The program also considers that amide protons too close to the paramagnetic ion become unobservable due to paramagnetic relaxation enhancements and takes the small correction terms into account that arise from residual anisotropic chemical shifts induced by paramagnetic alignment with the magnetic field.¹¹

If the 3D structure of the protein is known and a selectively ^{15}N -labeled protein sample is available, the $\Delta\chi$ tensor parameters can also be determined together with the assignments of the paramagnetic and diamagnetic ^{15}N HSQC cross-peaks using the program Platypus.³⁵ Since the ^{15}N HSQC spectrum of a selectively ^{15}N -labeled protein contains only few cross-peaks, it allows the unambiguous measurement of a significant number of PCSs (Figure 1b). The assignments are subsequently obtained from the best fit between experimental and predicted PCSs found in an exhaustive grid search over all possible $\Delta\chi$ tensor orientations and physically reasonable magnitudes, which consider any plausible assignment of the cross-peaks to specific residues of the protein.³⁵

Application I: Fast Structure Determination of a Protein–Protein Complex

PCSs measured in ^{15}N HSQC spectra have successfully been used for the structure determination of a 30 kDa complex between two proteins from the *Escherichia coli* replisome, the N-terminal domain $\epsilon 186$ of the proofreading exonuclease and the subunit θ .²⁷ The NMR structure of θ in complex with $\epsilon 186$ was determined by conventional 3D triple-resonance experiments.³⁶ The crystal structure of $\epsilon 186$ ³⁷ showed the presence of a binding site for Mg^{2+} or Mn^{2+} , which could also bind a single lanthanide ion with micromolar affinity (A. Y. Park, personal communication). Samples with selectively ^{15}N -leucine- and ^{15}N -phenylalanine-labeled $\epsilon 186$ were used to determine the $\Delta\chi$ tensors of Dy^{3+} and Er^{3+} with respect to $\epsilon 186$ and uniformly $^{15}\text{N}/^{13}\text{C}$ -labeled θ provided the $\Delta\chi$ tensors with respect to θ . Since the $\Delta\chi$ tensors determined for $\epsilon 186$ and θ arose from the same metal ion bound to $\epsilon 186$, superposition of the tensors determined for the two proteins yielded the structure of the complex in a single step of rigid body docking (Figure 4). The result was in full agreement with intermolecular nuclear Overhauser effects (NOEs) detected in 3D nuclear Overhauser effect spectroscopy (NOESY)– ^{15}N HSQC spectra. Repetition of the docking procedure with slightly varied parameters to

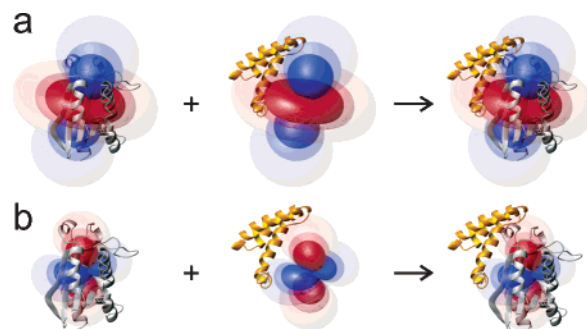


FIGURE 4. Rigid body docking of the proteins $\epsilon 186$ and θ by superposition of the $\Delta\chi$ tensors of Dy^{3+} and Er^{3+} determined with respect to the individual proteins. The $\Delta\chi$ tensors are represented by PCS isosurfaces with positive and negative shifts indicated by blue and red colors, respectively. The 3D structures of $\epsilon 186$ and θ are represented by gray and yellow ribbons. The positions and orientations of the $\Delta\chi$ tensors with respect to the individual proteins were experimentally determined from PCSs observed with samples where either $\epsilon 186$ or θ was ^{15}N -labeled: (a) PCS isosurfaces induced by Dy^{3+} on $\epsilon 186$, θ , and the $\epsilon 186/\theta$ complex; (b) same as panel a, except for isosurfaces induced by Er^{3+} .

reflect the experimental uncertainties resulted in a family of complex structures, most of which showed no clashes between backbone atoms.²⁷

Since the $\Delta\chi$ tensor of a single lanthanide ion is symmetric with respect to the x , y , and z axis (Figure 2b), data from a single lanthanide ion would lead to four different, fully equivalent ways in which the tensors observed in the two proteins can be superimposed. Some of these solutions would locate the two proteins too close or too far from each other to be acceptable. A better approach to resolving these ambiguities, however, is presented by the use of two different lanthanide ions with two differently oriented $\Delta\chi$ tensors, as generated by Dy^{3+} and Er^{3+} . Data from two differently oriented $\Delta\chi$ tensors result in a single docking solution (Figure 4).

Application II: Fast Determination of the Binding Mode of a Small Ligand

The paramagnetic effects from lanthanide ions can also be harnessed for the determination of the 3D structure of a small ligand molecule bound to its protein target in solution and, simultaneously, its location and orientation with respect to the protein. The principle has been demonstrated for thymidine bound to $\epsilon 186/\theta$ loaded with Dy^{3+} , Tb^{3+} , or Er^{3+} .²⁸

Thymidine binds only weakly to $\epsilon 186$, with a dissociation constant of about 7 mM. Therefore, the exchange between bound and free thymidine is fast on the NMR time scale (i.e., within milliseconds or less), and the NMR signals observed for thymidine are averaged between both environments. With a paramagnetic Ln^{3+} ion bound to $\epsilon 186$, concentration-dependent relaxation enhancements and PCSs were observed (Figure 5) from which the binding affinity and, hence, fraction of bound thymidine could readily be derived. This allowed the calculation of the PCSs in the bound form from the much smaller values experimentally observed in the average NMR spectra. (Notably,

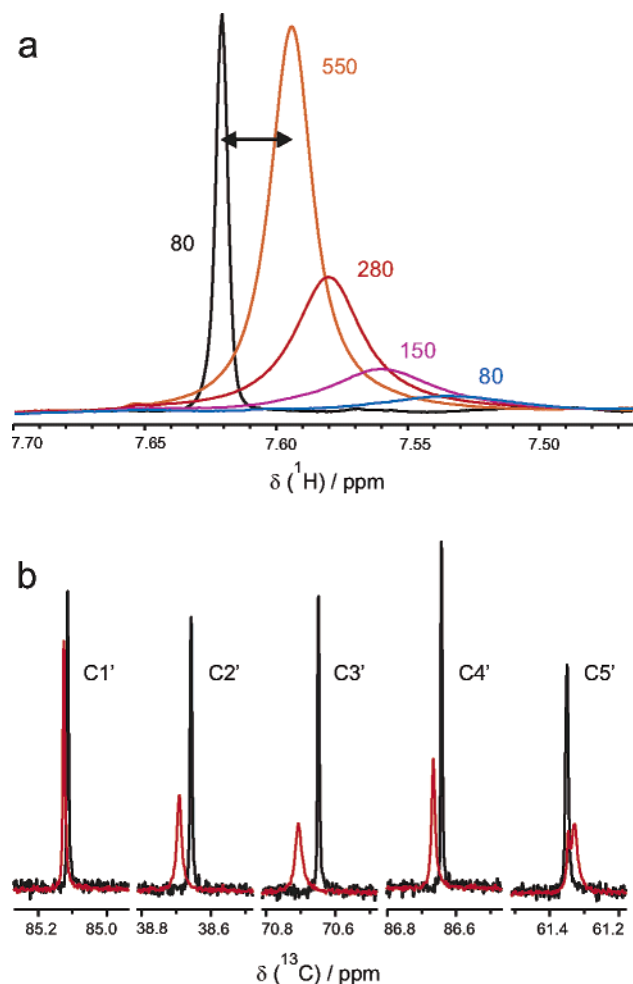


FIGURE 5. ^1H and ^{13}C NMR resonances of thymidine in the presence of diamagnetic $\epsilon 186/\theta/\text{La}^{3+}$ (black) and paramagnetic $\epsilon 186/\theta/\text{Tb}^{3+}$ (colored): (a) ^1H NMR resonance of the H6 proton of thymidine at increasing thymidine concentrations. The spectra are labeled with the ligand/protein ratio. The binding affinity of thymidine can be derived from the concentration dependence of the paramagnetic shifts and line broadenings, yielding the values of shifts and broadenings in the complex. (b) ^{13}C NMR resonances of the deoxyribose moiety of thymidine at 550-fold excess of thymidine, illustrating different line broadening and PCSs for ^{13}C spins located at different positions with respect to the $\Delta\chi$ tensor. The signal of C5' overlaps with a small signal from buffer.

straightforward 1D ^1H and ^{13}C NMR spectra were sufficient to record the PCSs of thymidine, because its NMR resonances were by far the strongest signals in the presence of a large excess of thymidine.)

Combined with the $\Delta\chi$ tensor of the lanthanide ion determined with respect to $\epsilon 186$ (see above), the PCS data of thymidine could be used to position its ^1H and ^{13}C nuclei with respect to the $\Delta\chi$ tensor and, hence, the $\epsilon 186$ molecule (Figure 6).²⁸ The structure and location of the thymidine molecule was found to be very similar to that determined for TMP in the single crystal.^{28,37} As in the case of protein–protein docking (see above), the four equivalent orientations of the thymidine molecule with respect to the $\Delta\chi$ tensor of a single lanthanide was reduced to a single solution by addition of PCS data from further Ln^{3+} ions with differently oriented $\Delta\chi$ tensors. Only in the case

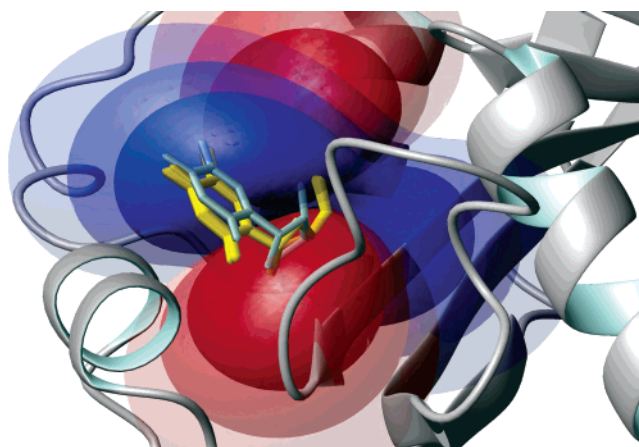


FIGURE 6. Structure of the $\epsilon 186/\text{thymidine}$ complex calculated with PCS data of thymidine. Pseudocontact shifts were measured for complexes with Dy^{3+} , Tb^{3+} , and Er^{3+} and used as input for a simulated annealing calculation with Xplor-NIH.^{53,54} The backbone of $\epsilon 186$ was kept rigid during the calculations, while the protein side chains and the thymidine starting conformations and positions were randomized. The results of seven calculations are shown (thymidine in yellow using a heavy-atom representation) overlaid onto the crystal structure of the $\epsilon 186/\text{TMP}$ complex³⁷ in gray and the $\Delta\chi$ tensor of Tb^{3+} represented by blue and red isosurfaces for positive and negative PCSs, respectively.

of nonchiral ligand molecules, data from differently oriented $\Delta\chi$ tensors would allow two equivalent solutions, which must be discriminated based on steric or other criteria.

Site-Specific Lanthanide Labeling

In the case where the protein does not contain a natural lanthanide binding site, methods are available by which a lanthanide binding site can be crafted onto a protein at strategic positions. One approach is based on N- or C-terminal fusion of a lanthanide-binding peptide (LBP), either using a peptide sequence known to bind Ca^{2+} or a peptide specifically evolved for high-affinity binding of lanthanide ions.^{38,39} This approach tends to generate only small PCSs in the protein of interest because of averaging of the $\Delta\chi$ tensor when the peptide tag moves with respect to the protein. In addition, the approach restricts the attachment of a lanthanide ion to the N- or C-terminus of the protein.

Both problems can be addressed by attaching the LBP via a disulfide bond to a single cysteine residue in the protein. Compared with flexible N- or C-terminal polypeptide segments, a disulfide bond presents a shorter, more rigid tether, and site-directed mutagenesis can be employed to produce a protein sample with a single cysteine residue at any strategically chosen site on the protein surface. A 16-residue LBP containing a cysteine residue can readily be made by chemical peptide synthesis and the disulfide bond with the protein of interest can be formed in high yields using Ellman's reagent for activation of the protein thiol group (Figure 7).⁴⁰ This is a generally applicable method for the attachment of thiol-containing compounds to cysteine side chains.⁴¹ Usually, the peptide

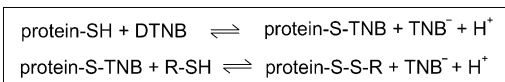


FIGURE 7. Covalent attachment of a thiol-compound to a protein cysteine side chain via a disulfide bond.⁴⁰ The cysteine thiol group is activated by Ellman's reagent, 5,5'-dithiobis(2-nitrobenzoic acid) (DTNB), resulting in a mixed disulfide bond with 5-mercapto-2-nitrobenzoic acid (TNB).⁴¹ The mixed disulfide with TNB is readily exchanged for a mixed disulfide with other thiol-containing compounds. Progress of the reaction can be monitored by the release of colored 5-mercapto-2-nitrobenzoate in both steps.

is not isotope labeled and does not appear in hetero-nuclear NMR spectra of isotope- and LBP-labeled proteins.

A variation of the above approach is presented by the use of chemically synthesized lanthanide-chelating tags (LCTs) with an activated thiol group. A commercially available tag based on EDTA has been shown to provide a high-affinity lanthanide binding site.^{42,43} This tag, however, coordinates lanthanide ions in a chiral fashion, so the association with a protein results in diastereomers.⁴⁴ In complex with metal ions with nonisotropic χ tensor, the diastereomers generate different $\Delta\chi$ tensor orientations and therefore induce different PCSs in the protein, resulting in peak doubling, increased spectral overlap, and assignment ambiguities.^{43,44} This can be avoided by the use of chiral LCTs, where the LCT diastereomers resulting from chiral metal ion coordination are of sufficiently different energy to lead to preferred population of a single conformer.^{44–46} Yet, due to the small size of LCTs, mobility of the disulfide tether between the LCT and the protein is a common phenomenon that reduces the observable PCSs by averaging.⁴⁷ The mobility problem has been addressed by a tag with attachment points for two cysteine residues, but multiple diastereomeric forms were observed in this particular case.⁴⁸ The synthesis of a readily accessible chiral LCT with specific lanthanide-binding mode and a short tether is a current challenge.

Concluding Remarks

Lanthanide labeling of proteins is set to become an important tool in structural biology for establishing 3D models of protein–protein complexes and in drug discovery for the analysis of the binding mode of small ligands to proteins. The PCS effects are long range, scalable by the choice of lanthanide ion, and easy to measure by the most sensitive NMR experiments available. The $\Delta\chi$ tensor required for back-calculation of PCS is fully characterized by only eight parameters, which can be derived from a corresponding number of experimental PCS values if the position of the respective nuclear spins with respect to the lanthanide ion is known. The $\Delta\chi$ tensor can thus be determined even if only few of the protein NMR signals are assigned, with additional assignments leading to correspondingly increased accuracy of the $\Delta\chi$ tensor, especially if the nuclear spins are distributed around the metal ion in all three directions of the coordinate system spanned by the $\Delta\chi$ tensor.

Prior knowledge of the 3D structure of the lanthanide-labeled protein opens exceptionally convenient routes for

resonance assignment of the paramagnetic NMR spectra, where available computer algorithms can be used to obtain the assignments and the $\Delta\chi$ tensor parameters simultaneously.^{34,35} Even the resonance assignment of the diamagnetic NMR signals can be determined in this way, if a selectively ¹⁵N-labeled protein sample is available. The required protein samples are inexpensive to prepare, because no ¹³C-labeling is required. In combination with perdeuteration, systems with >100 kDa molecular weight will be amenable to this approach, since 2D ¹⁵N–¹H correlation spectra suffice for PCS measurements.

In the case of small, transiently binding ligand molecules, even 1D ¹H and ¹³C NMR spectra at natural isotopic abundance can be sufficient for PCS measurements. The use of ¹³C NMR data is of particular interest in drug discovery, where more information may be gleaned from the ¹³C than from the ¹H NMR spectrum due to greater abundance of carbon than hydrogen in the molecule and better resolution of the ¹³C NMR spectrum. ¹³C spins are also less sensitive to paramagnetic relaxation enhancements due to their smaller gyromagnetic ratio.⁷ In situations, where the structure of the protein–ligand complex cannot be determined by X-ray crystallography, PCS data may deliver more detailed information about the ligand binding mode with less effort than any other technique.

Ongoing efforts in our laboratory attempt to combine site-specific lanthanide labeling with cell-free protein synthesis, which is a particularly fast and inexpensive method for the preparation of selectively ¹⁵N-labeled proteins.⁴⁹ While this review focused on PCSs as one of the most striking NMR features of lanthanide ions, greater use will also be made of the structural information contained in cross-correlation effects, relaxation enhancements, and residual dipolar couplings associated with the paramagnetism of lanthanide ions.^{7,18,35} Considering finally that lanthanide ions also possess highly unusual and attractive electronic and luminescent properties,^{50,51} lanthanide-labeled proteins carry great potential in many areas of biological research.

The authors thank Professor Nicholas E. Dixon and his group members for the continued supply of isotope-labeled samples and Dr. Thomas Huber for computer programs.

References

- (1) McConnell, H. M.; Robertson, R. E. Isotropic nuclear resonance shifts. *J. Chem. Phys.* **1958**, *29*, 1361–1365.
- (2) Bleaney, B. Nuclear magnetic resonance shifts in solution due to lanthanide ions. *J. Magn. Reson.* **1972**, *8*, 91–100.
- (3) Hinckley, C. C. Paramagnetic shifts in solutions of cholesterol and the dipyrindine adduct of trisdipivalomethanatoeuropium(III). A shift reagent. *J. Am. Chem. Soc.* **1969**, *91*, 5160–5162.
- (4) Reuben, J. Paramagnetic lanthanide shift reagents in NMR spectroscopy: Principles, methodology and applications. *Prog. NMR Spectrosc.* **1973**, *9*, 3–70.
- (5) Geraldes, C. F. G. C. Lanthanide shift-reagents. *Methods Enzymol.* **1993**, *227*, 43–78.
- (6) Peters, J. A.; Huskens, J.; Raber, D. J. Lanthanide induced shifts and relaxation rate enhancements. *Prog. NMR Spectrosc.* **1996**, *28*, 283–350.
- (7) Bertini, I.; Luchinat, C.; Parigi, G. Magnetic susceptibility in paramagnetic NMR. *Prog. NMR Spectrosc.* **2002**, *40*, 249–273.

- (8) Tolman, J. R.; Flanagan, J. M.; Kennedy, M. A.; Prestegard, J. H. Nuclear magnetic dipole interactions in field-oriented proteins: information for structure determination in solution. *Proc. Natl. Acad. Sci. U.S.A.* **1995**, *92*, 9279–9283.
- (9) Pintacuda, G.; Hohenthanner, K.; Otting, G.; Müller, N. Angular dependence of dipole-dipole-Curie-spin cross-correlation effects in high-spin and low-spin paramagnetic myoglobin. *J. Biomol. NMR* **2003**, *27*, 115–132.
- (10) Pintacuda, G.; Kaikkonen, A.; Otting, G. Modulation of the distance dependence of paramagnetic relaxation enhancements by CSAxDSA cross-correlation. *J. Magn. Reson.* **2004**, *171*, 233–243.
- (11) John, M.; Park, A. Y.; Pintacuda, G.; Dixon, N. E.; Otting, G. Weak alignment of paramagnetic proteins warrants correction for residual CSA effects in measurements of pseudocontact shifts. *J. Am. Chem. Soc.* **2005**, *127*, 17190–17191.
- (12) Barry, C. D.; North, A. C. T.; Glasel, J. A.; Williams, R. J. P.; Xavier, A. V. Quantitative determination of mononucleotide conformations in solution using lanthanide ion shift and broadening NMR probes. *Nature* **1971**, *232*, 236–245.
- (13) Lee, L.; Sykes, B. D. Use of lanthanide-induced nuclear magnetic resonance shifts for determination of protein structure in solution: EF calcium binding site of carp parvalbumin. *Biochemistry* **1983**, *22*, 4366–4373.
- (14) Senn, H.; Wüthrich, K. Amino-acid sequence, hem-iron coordination geometry and functional properties of mitochondrial and bacterial c-type cytochromes. *Q. Rev. Biophys.* **1985**, *18*, 111–134.
- (15) Ubbink, M.; Ejdebäck, M.; Karlsson, B. G.; Bendall, D. S. The structure of the complex of plastocyanin and cytochrome *f*, determined by paramagnetic NMR and restrained rigid-body molecular dynamics. *Structure* **1998**, *6*, 323–335.
- (16) Tu, K.; Gochin, M. Structure determination by restrained molecular dynamics using NMR pseudocontact shifts as experimentally determined constraints. *J. Am. Chem. Soc.* **1999**, *121*, 9276–9285.
- (17) Gochin, M.; Roder, H. Protein structure refinement based on paramagnetic NMR shifts: applications to wild-type and mutant forms of cytochrome *c*. *Protein Sci.* **1995**, *4*, 296–305.
- (18) Bertini, I.; Luchinat, C.; Parigi, G. Paramagnetic constraints: an aid for quick solution structure determination of paramagnetic metalloproteins. *Concepts Magn. Reson.* **2002**, *14*, 259–286.
- (19) Gaponenko, V.; Sarma, S. P.; Altieri, A. S.; Horita, D. A.; Li, J.; Byrd, R. A. Improving the accuracy of NMR structures of large proteins using pseudocontact shifts as long-range restraints. *J. Biomol. NMR* **2004**, *28*, 205–212.
- (20) Bertini, I.; Luchinat, C.; Parigi, G.; Pierattelli, R. NMR spectroscopy of paramagnetic metalloproteins. *ChemBioChem* **2005**, *6*, 1536–1549.
- (21) Bentrop, D.; Bertini, I.; Cremonini, M. A.; Forsén, S.; Luchinat, C.; Malmendal, A. Solution structure of the paramagnetic complex of the N-terminal domain of calmodulin with two Ce³⁺ ions by ¹H NMR. *Biochemistry* **1997**, *36*, 11605–11618.
- (22) Bertini, I.; Janik, M. B. L.; Lee, Y.-M.; Luchinat, C.; Rosato, A. Magnetic susceptibility tensor anisotropies for a lanthanide ion series in a fixed protein matrix. *J. Am. Chem. Soc.* **2001**, *123*, 4181–4188.
- (23) Biekofsky, R. R.; Muskett, F. W.; Schmidt, J. M.; Martin, S. R.; Browne, J. P.; Bayley, P. M.; Feeney, J. NMR approaches for monitoring domain orientations in calcium-binding proteins in solution using partial replacement of Ca²⁺ by Tb³⁺. *FEBS Lett.* **1999**, *460*, 519–526.
- (24) Mustafi, S. M.; Mukherjee, S.; Chary, K. V. R.; Del Bianco, C.; Luchinat, C. Energetics and mechanism of Ca²⁺ displacement by lanthanides in a calcium binding protein. *Biochemistry* **2004**, *43*, 9320–9331.
- (25) Gay, G. L.; Lindhout, D. A.; Sykes, B. D. Using lanthanide ions to align troponin complexes in solution: order of lanthanide occupancy in cardiac troponin C. *Protein Sci.* **2004**, *13*, 640–651.
- (26) Bertini, I.; Del Bianco, C.; Gelis, I.; Katsaros, N.; Luchinat, C.; Parigi, G.; Peana, M.; Provenzani, A.; Zoroddu, M. A. Experimentally exploring the conformational space sampled by domain reorientation in calmodulin. *Proc. Natl. Acad. Sci. U.S.A.* **2004**, *101*, 6841–6846.
- (27) Pintacuda, G.; Park, A. Y.; Keniry, M. A.; Dixon, N. E.; Otting, G. Lanthanide labeling offers fast NMR approach to 3D structure determinations of protein-protein complexes. *J. Am. Chem. Soc.* **2006**, *128*, 3696–3702.
- (28) John, M.; Pintacuda, G.; Park, A. Y.; Dixon, N. E.; Otting, G. Structure determination of protein–ligand complexes by transferred paramagnetic shifts. *J. Am. Chem. Soc.* **2006**, *128*, 12910–12916.
- (29) Allegrozzi, M.; Bertini, I.; Janik, M. B. L.; Lee, Y.-M.; Liu, G.; Luchinat, C. Lanthanide-induced pseudocontact shifts for solution structure refinements of macromolecules in shells up to 40 Å from the metal ion. *J. Am. Chem. Soc.* **2000**, *122*, 4154–4161.
- (30) Corson, D. C.; Williams, T. C.; Sykes, B. D. Calcium binding proteins: optical stopped-flow and proton nuclear magnetic resonance studies of the binding of the lanthanide series of metal ions to parvalbumin. *Biochemistry* **1983**, *22*, 5882–5889.
- (31) Nitz, M.; Sherawat, M.; Franz, K. J.; Peisach, E.; Allen, K. N.; Imperiali, B. Structural origin of the high affinity of a chemically evolved lanthanide-binding peptide. *Angew. Chem., Int. Ed.* **2004**, *43*, 3682–3685.
- (32) Bottrill, M.; Kwok, L.; Long, N. J. Lanthanides in magnetic resonance imaging. *Chem. Soc. Rev.* **2006**, *35*, 557–571.
- (33) Pintacuda, G.; Otting, G. Identification of protein surfaces by NMR measurements with a paramagnetic Gd(III) chelate. *J. Am. Chem. Soc.* **2002**, *124*, 372–373.
- (34) Schmitz, C.; John, M.; Park, A. Y.; Dixon, N. E.; Otting, G.; Pintacuda, G.; Huber, T. Efficient χ -tensor determination and NH assignment of paramagnetic proteins. *J. Biomol. NMR* **2006**, *35*, 79–87.
- (35) Pintacuda, G.; Keniry, M. A.; Huber, T.; Park, A. Y.; Dixon, N. E.; Otting, G. Fast structure-based assignment of ¹⁵N HSQC spectra of selectively ¹⁵N-labeled paramagnetic proteins. *J. Am. Chem. Soc.* **2004**, *126*, 2963–2970.
- (36) Keniry, M. A.; Park, A. Y.; Owen, E. A.; Hamdan, S. M.; Pintacuda, G.; Otting, G.; Dixon, N. E. Structure of the θ subunit of *Escherichia coli* DNA polymerase III in complex with the ϵ subunit. *J. Bacteriol.* **2006**, *188*, 4464–4473.
- (37) Hamdan, S.; Carr, P. D.; Brown, S. E.; Ollis, D. L.; Dixon, N. E. Structural basis for proofreading during replication of the *Escherichia coli* chromosome. *Structure* **2002**, *10*, 535–546.
- (38) Ma, C.; Opella, S. J. Lanthanide ions bind specifically to an added “EF-hand” and orient a membrane protein in micelles for solution NMR spectroscopy. *J. Magn. Reson.* **2000**, *146*, 381–384.
- (39) Wöhnert, J.; Franz, K. J.; Nitz, M.; Imperiali, B.; Schwalbe, H. Protein alignment by a coexpressed lanthanide-binding tag for the measurement of residual dipolar couplings. *J. Am. Chem. Soc.* **2003**, *125*, 13338–13339.
- (40) Su, X.-C.; Huber, T.; Dixon, N. E.; Otting, G. Site-specific labelling of proteins with a lanthanide-binding tag. *ChemBioChem* **2006**, *7*, 1599–1604.
- (41) Jocelyn, P. C. Spectrophotometric assay of thiols. *Methods Enzymol.* **1987**, *143*, 44–67.
- (42) Dvoretzky, A.; Gaponenko, V.; Rosevear, P. R. Derivation of structural restraints using a thiol-reactive chelator. *FEBS Lett.* **2002**, *528*, 189–192.
- (43) Pintacuda, G.; Moshref, A.; Leonchiks, A.; Sharipo, A.; Otting, G. Site-specific labelling with a metal chelator for protein-structure refinement. *J. Biomol. NMR* **2004**, *29*, 351–361.
- (44) Ikegami, T.; Verdier, L.; Sakhaii, P.; Grimme, S.; Pescatore, B.; Saxena, K.; Fiebig, K. M.; Griesinger, C. Novel techniques for weak alignment of proteins in solution using chemical tags coordinating lanthanide ions. *J. Biomol. NMR* **2004**, *29*, 339–349.
- (45) Leonov, A.; Voigt, B.; Rodriguez-Castañeda, F.; Sakhaii, P.; Griesinger, C. Convenient synthesis of multifunctional EDTA-based chiral metal chelates substituted with an S-mesylcysteine. *Chem.–Eur. J.* **2005**, *11*, 3342–3348.
- (46) Haberb, P.; Rodriguez-Castañeda, F.; Junker, J.; Becker, S.; Leonov, A.; Griesinger, C. Two new chiral EDTA-based metal chelates for weak alignment of proteins in solution. *Org. Lett.* **2006**, *8*, 1275–1278.
- (47) Rodriguez-Castañeda, F.; Haberb, P.; Leonov, A.; Griesinger, C. Paramagnetic tagging of diamagnetic proteins for solution NMR. *Magn. Reson. Chem.* **2006**, *44*, S10–S16.
- (48) Prudêncio, M.; Rohovec, J.; Peters, J. A.; Tocheva, E.; Boulanger, M. J.; Murphy, M. E. P.; Hupkes, H.-J.; Kusters, W.; Impagliazzo, A.; Ubbink, M. A caged lanthanide complex as a paramagnetic shift agent for protein NMR. *Chem.–Eur. J.* **2004**, *10*, 3252–3260.
- (49) Ozawa, K.; Wu, P. S. C.; Dixon, N. E.; Otting, G. ¹⁵N-Labelled proteins by cell-free protein synthesis: strategies for high-throughput NMR studies of proteins and protein-ligand complexes. *FEBS J.* **2006**, *273*, 4154–4159.
- (50) Di Bari, L.; Salvadori, P. Solution structure of chiral lanthanide complexes. *Coord. Chem. Rev.* **2005**, *249*, 2854–2879.
- (51) Bünzli, J. C.-G. Benefiting from the unique properties of lanthanide ions. *Acc. Chem. Res.* **2006**, *39*, 53–61.
- (52) Alsaadi, B. M.; Rossetti, F. J. C.; Williams, R. J. P. Electron relaxation rates of lanthanide aquo-cations. *J. Chem. Soc., Dalton Trans.* **1980**, 2147–2150.
- (53) Schwieters, C. D.; Kuszewski, J. J.; Tjandra, N.; Clore, G. M. The Xplor-NIH NMR molecular structure determination package. *J. Magn. Reson.* **2003**, *160*, 65–73.
- (54) Banci, L.; Bertini, I.; Cavallaro, G.; Giachetti, A.; Luchinat, C.; Parigi, G. Paramagnetism-based restraints for Xplor-NIH. *J. Biomol. NMR* **2004**, *28*, 249–261.

AR050087Z